FATIGUE IN WELDED CONSTRUCTIONS

H.-P. LIEURADE *

Abstract

For some time now, the concern for improving the lightness of steel structures, coupled with the increase in applied operating stresses, has encouraged design engineers to take an interest in the fatigue of the structures designed by them, which sometimes fail as a result of poor welded joint selection.

In order to study the fatigue characteristics of a structure subjected to a cyclic load amplitude, the structure must frequently be broken down into a number of welded joints.

The present paper outlines, for welded structures, the process of failure for various types of welded joint, following which the influence of certain technological and mechanical parameters on welded-joint fatigue strength is shown. The paper then demonstrates that weld fatigue characteristics can be improved by certain heat treatment or mechanical treatment operations.

1. INTRODUCTION

Welding is at present the main method of steel-structure fabrication. Without welding, many industrial applications would have been unfeasible.

Based on the observation of numerous operating failures of welded structures, fatigue usually appears as the main cause of failure. Moreover, in the case of welded structures it soon became clear that admissible operating stresses were very slight by comparison with static stresses (yield strength, ultimate tensile strength) and that it is not sufficient to apply a safety factor based, for example, on a fraction of the yield strength in order to be certain of preventing operating failure. Welds may set up severe stress concentrations which vary from one construction detail to another.

On the other hand, if a safety factor sufficiently great to eliminate any possibility of failure is allowed for, then the welded structure becomes oversized and is uncompetitive.

* Institut de Recherches de la Sidérurgie Française (IRSID)
Saint-Germain-en-Laye Cedex (France).

Finally, in designing a structure, each structural member should comply with the following three conditions.
- The member should perform its function as efficiently as possible.
- It should allow economical manufacturing.
- The member should provide a defined service life.

As a consequence of the first two conditions, safety factors are reduced during designing, so as to reduce the weight and cost. Unfortunately, this trend is detrimental to satisfactory member lifetime and accordingly the safety of the structure, in the event that damage due to fatigue may occur.

Moreover, the fatigue strength of real structures cannot be described in a purely theoretical manner. This is why the only realistic approach for the design of a structure subjected to fatigue stresses is to compare the applied stress rates with the fatigue strength characteristics corresponding to the configurations of each joint used.

For this purpose, standards or recommendations exist in all countries. The codes, however, are applicable only to specific types of steel structures.

The object of the present paper is not to set out exhaustively the results contained in the literature on this subject, but to provide a schematic analytical outline of the main parameters affecting the fatigue strength of welded joints. At the same time, the paper outlines the main methods allowing an improvement in the fatigue strength of such joints.

2. FATIGUE FAILURE OF MAIN WELDED JOINTS

The welding process sets up stress concentration areas from which a fatigue crack can be initiated and subsequently propagated. These areas correspond either to a geometrical irregularity of the weld bead, or defects, whether internal (incomplete root penetration, porosity) or external (undercuts, slag inclusions). The relative size of such areas depends on the type of joint.

2.1 Butt welds

Transverse butt welds

This type of joint, which allows two plates to be connected together by a transverse weld perpendicular to the axis of stress, is shown in figure 1.

For this type of joint, the fatigue crack is initiated at the weld toe and is propagated through the thickness of the plate, normally in the direction of loading. The crack is accordingly not the result of a defective weld or poor filler-metal properties, but the consequence of stress concentration in the weld toe.

On this type of welded joint, the shape of the weld bead has a major influence on the butt joint's fatigue characteristics. The weld shape depends to a large extent on welding conditions.

Longitudinal butt welds

For longitudinal joints, the change in cross-section due to excess metal is parallel to the direction of the stress applied. Now, it might be

thought that the fatigue characteristics of such welds would be better than those of tranverse joints, but this is not the case.

Cracking on this type of joint is generally initiated (figure 2) where welding has been stopped and then resumed, e.g. for changing an electrode, or else from a fold on the surface of the weld bead.

Good longitudinal-joint fatigue strength can be obtained only if the joints are continuous and if weld end effect can be avoided.

2.2 Fillet welded joints

Cruciform joints

There are two types of cruciform joint, defined according to whether or not the weld beads transmit stress.

Non-load-carrying cruciform joints. In the first type of cruciform joint (figure 3), the fillet weld does not transmit the stress through the continuous core. In this case, the crack is initiated at the weld toe and is propagated through the thickness of the plate in a plane perpendicular to the plane of stress.

There is no advantage in executing joints by fillet welds parallel to the direction of the stress (figure 4). The crack is in this case initiated at the end of the bead, resulting in the same fatigue strength as for transverse fillet joints. Continuous longitudinal fillet welds, on the other hand, provide a major improvement in fatigue life by comparison with intermittent fillet welds.

Load-carrying cruciform joints. For this type of joint, all stresses are transmitted through the weld (figure 5).

In this case, in addition to the stress concentration areas located in the weld toe, there are areas of acute internal notching located at the root of the weld. Generally, cracks are initiated at this point, being subsequently propagated through the filler metal in an oblique direction relative to the direction of stress.

This type of fracture mode results in relatively low joint fatigue characteristics by comparison with the aforementioned welded joints. That is why an endeavour is usually made to avoid crack initiation at the root of the weld. However, increasing the groove thickness by means of a thicker weld or improved penetration is not always sufficient to ensure that fatigue cracks will be initiated from the weld toe. Generally, full bead penetration is practised (figure 6), with the result of approximately doubling the fatigue limit.

Harrison (1) has shown that full penetration is not necessary in order to shift from crack initiation at the weld root to initiation at the weld toe. Figure 7 shows the weld shape conditions necessary to shift from one type of fracture to the other.

Tee joints

At first sight, this joint resembles a semi-cruciform joint (figure 8) and should show similar fatigue characteristics. However, in this case, a third fracture mode is possible. If the bending stresses induced in the transverse member are of the same order of magnitude as the stresses

applied directly on the Tee, the crack may be initiated in the other weld toes and will be propagated through the transverse member.

3. WELDED-JOINT FATIGUE FACTORS

The static strength of a butt joint is usually equal to the strength of the base metal, with failure occurring outside the weld bead (unless the weld is itself very poor). However, the fatigue strength of the welded joint is always lower and failure almost always occurs at the level of the weld bead (cf. section 2.1). The fatigue strength of welded joints is affected by various parameters.

Geometric factors

Such factors are the weld shape, plate misalignment, deflection of the welded member, and the joint size (plate thickness, weld-bead dimensions).

Metallurgical factors

Such factors are the nature of the base metal, the welding process (energy, filler metal), welding defects, and the residual stress level.

Stress-related factors

Such factors are the loading mode (constant or variable amplitude, loading ratio), the stress gradient, stress biaxiality, and the environment.

Each of these many factors generally does not act alone. Synergic effects often have to be allowed for, thereby complicating the choice of an acceptable operating stress level.

3.1 Concept of nominal stress

An elementary welded joint can be regarded as a notched structural member, with the weld bead forming the notch. As in the case of a notched member, the nominal stress range $\Delta\sigma_N$ at the initiation point will be considered. Figure 9 shows $\Delta\sigma_N$ in the case of a joint with transverse stiffener subjected to either tensile or bending stress.

Sometimes, the nominal stress gradient may be non-linear, as in the case, for example, of tubular joints. For such joints, the evolution of the gradient in the vicinity of the "hot spot" must be defined correctly, i.e., without allowing for the additional gradient due to the notch effect induced by the weld toe (figure 10).

In such cases, finite element calculations must be performed, or else measurements must be made by strain gauges on models or full-scale joints (2).

Generally, $\Delta\sigma_N$ is transferred onto the Wöhler's Charts ($\Delta\sigma_N$ - N_R), in order to plot the so-called "S-N" curves.

As will be seen further on, the conventional fatigue limit at 2×10^6 cycles is often adopted as a reference. By way of example, figure 11 shows, for a few types of joint, the acceptable stress levels proposed by the International Institute of Welding (3). Note the relatively low values by comparison with the base metal yield strength ($\sigma_Y \geq 240$ MPa). In practice, these acceptable stress values are a translation of the wide

spread of test results on welded joints in the as-welded condition, due to the effect of the many parameters mentioned above.

3.3 Geometric factors

3.2.1 Weld bead shape

The overall influence of weld bead shape can be shown by comparing the fatigue limits obtained, on the one hand on as-welded butt joints, and on the other hand on the same welded joints machined flush.

For joints machined flush ,the fatigue limit found is slightly (5 to 10%) below that of the base metal, whereas the fatigue limit observed on as-welded joints is well below that of the base metal (by 30 to 45%).

In reality, as several authors have shown, allowance must be made for the macrogeometric effect due to the general weld profile, and the microscopic effect induced by the weld flaws located in the transition zone between the surface of the weld bead and the skin of the base metal.

Macrogeometric effect. Due to the nature of the welded joints, the weld beads induce cross-sectional changes which lead to the appearance of stress concentrations (figure 12).

By photoelastometric measurements, Kenyon, Morrison and Quarrell (5) measured, on fillet joints at the point of transition between the weld bead and the base metal, values of the stress concentration factor ranging between 1.5 and 4.5. For butt welds, this factor is around 3. The measurements do not take into account the presence of possible defects at the point examined, which cause local increases in this stress concentration.

Lawrence (6) has performed finite element calculations to determine the values of butt-weld stress concentration factor K_t as a function of various weld shape parameters.

To illustrate the influence of weld shape, various systematic studies were carried out, comparing the fatigue strength of welded joints with that of machined test pieces of similar profile to the welded test pieces (7), (8). In this way, it is possible to continuously vary radius ρ and the transition angle θ of the joint simulated (figure 13). The studies showed that an increase in ρ or a reduction in θ increase the fatigue limit. The influence of ρ becomes insignificant when θ is less than 10 or 15°, and the influence of θ becomes insignificant either when its value exceeds 40° or when ρ exceeds 6 to 10 mm.

Nishida (9) has proposed an expression of stress concentration factor K_t as a function of weld shape parameters, for a number of typical welded joints.

Several authors (10), (11), have studied the influence of weld shape directly on welded joints. In particular, Richards has shown that the fatigue limit increases in proportion to the weld bead transition angle (figure 14) on a butt weld.

Microgeometric effect. In addition to stress concentrations due to cross-sectional changes, through defects such as cracks, undercuts or misalignment, etc., all represent so many potential incipient fractures.

For high-strength steels, F. Watkinson et al. (12) have shown that the low fatigue strength of welded joints on high-yield-strength steels could be explained by the presence of very acute defects. The researchers carried out tests on test pieces with an artificial notch of 0.12 mm depth and radius 0.012 mm on the weld toe. The results obtained on these test pieces come within the spread of the test results obtained on unmachined test pieces.

In actual fact, Petershagen (13) has shown that it is hard to quantify the effect of an undercut on the fatigue strength of welded joints, since measuring the depth and acuity of an undercut is a very tricky job. Figure 15 shows, for the case of butt welds, a major fall in $\Delta\sigma$ with h/t (where h = undercut depth and t = plate thickness).

3.2.2 Plate thickness

Many studies have shown that for geometrically similar joints, the fatigue strength tends to decrease as plate thickness increases (14).

However, it is very difficult to distinguish experimentally the effect of the transition angle, θ, from the underbead length, s, and plate thickness, t. For a given configuration, as s/t decreases, $\Delta\sigma_N$ increases as shown in figure 16 (15).

Instead of s, allowance should no doubt be made for the length of the plate fit conferred by the welded joint (16) (2s + stiffener thickness).

A similar effect is allowed for in calculating tubular welded joints for which this effect is very marked (figure 17). The following relation is used in the offshore construction industry (17):

$$S = S^* \left(\frac{T}{18}\right)^{0.29} \qquad (1)$$

Where:

S_* = acceptable stress range for the joint in question
S = stress range calculated on the basis of the S-N curve, and
T = member thickness

3.2.3 Misalignment

Figure 18 shows various misalignments, either axial or angular, which may be found in welded joints. These types of defect result in parasitic bending moments which are added to the nominal stress applied.

The increase in nominal stress due to an axial alignment defect, δ, can be calculated by the following relation (18):

$$K_t = 1 + 3\frac{\delta}{e_1}\left(\frac{2e_1^3}{e_1^3 + e_2^3}\right) \qquad (2)$$

Where: e_1 and e_2 are the thicknesses of the respective welded plates.

The combined effect of the two types of alignment defect (axial and angular) is allowed for in the DnV regulations dealing with offshore structures (19).

3.3 Metallurgical factors

3.3.1 Internal defects

The influence of incomplete root penetration has been determined by Newman (20), who has shown that the fall in fatigue strength was proportionate to the length of the defect. Newman also showed (21) that a relation could be established between this fall and the cross-sectional reduction caused by the defect.

The influence of inclusions and slag lines has been studied on a systematic basis by the British Welding Research Association (22), (23). One of the main conclusions reached is that the detrimental effect of the defect depends chiefly on the possible presence of hydrogen. The role of hydrogen in the fall in welded-joint fatigue strength, in conjunction with the presence of defects and porosities, has been recognized by many authors (24), (25), (26).

The influence of porosity (figure 19) and slag inclusions (figure 20) on fatigue characteristics has been determined by Ishii et al. (27). For tests at constant loading amplitude, these researchers have shown that such defects, even when large, affected the metal's fatigue strength for lifetimes longer than 10^4 cycles.

A bibliographic survey (28) has shown that the volume percentage of blowholes could be related to various qualities of weld.

More generally, by a statistical study of the influence of defects in weld constructions, Matting and Neitzel (29) have shown that the extent of the defects' detrimental influence (pores, restarting craters, incomplete root penetration, nonmetallic inclusions, and undercuts) corresponds to the stress concentration applied.

3.3.2 Residual stresses

By definition, residual stresses form a system of internal stresses, in equilibrium, which exists in the absence of external loading. Such stresses are usually the result of a permanent plastic deformation which locally causes additional deformation and subsequent stresses at other points.

In a welded structure, such deformations are the result of local heating and cooling cycles associated with the welding process and, in particular, with the metal's contraction. When the welded metal cools down from the fusion temperature, it tends to contract, but is held back by the base metal in the vicinity. This contraction must then be accommodated by plastic deformation of the filler metal.

This situation is complicated still further by technological factors such as the joint type and size, the welding process used, and the method of depositing the filler metal. However, the principle of the existence of major residual stresses in the filler metal remains the same. In the case of multipass or high-energy welding, these residual stresses may reach the level of the plate's yield strength in the vicinity of the fatigue crack initiation point. Figure 21 gives an example of such stresses in the case of a transverse joint. When the welded joint is placed under load, this residual stress field is added to the dynamic stresses, with a proportionate reduction in the fatigue strength of the structure subjected to stress.

3.3.3 Welding processes

Generally speaking, a welding process will give improved joint fatigue strength insofar as it results in:
- few small defects (12) (TIG welding, submerged arc welding);
- slight residual stresses;
- a weld bead with a small transition angle (automatic welding).

Figure 22 shows the results of tests carried out at the IRSID on test pieces in E36 steel, welded manually, with a convex bead, and test pieces in the same steel fabricated by automatic submerged arc welding (SAW), with a concave bead. The fatigue strength of test pieces fabricated by automatic welding is approximately 40% greater than that of manually welded test pieces.

In actual fact, the preparation of the welding operation plays a more decisive role than the welding process in welded-joint fatigue strength. In particular, in the case of an automatic welding process, the selection of optimum welding parameters with respect to fatigue strength is an essential factor.

3.3.4 Nature of the base metal and filler metal

Obviously, the choice of filler metal depends on the nature of the base metal to be welded. In selecting the filler metal, the following points should be taken into account.

- The filler metal (electrodes, filler rod) should make it possible to obtain filler-metal mechanical properties compatible with those of the base metal, so as to ensure good continuity of properties.

- Preferably, the filler metal selected should give off little or no hydrogen (e.g., stove-baked basic electrodes).

By obtaining, for cruciform joints, complete penetration between the filler metal and the base metal, without any break in continuity at the centre and with concave beads, a fatigue strength close to that of butt welds can be obtained. Such conditions can be obtained by selecting deep-penetration electrodes for the first passes and improved coated electrodes for the final passes.

In the course of tests carried out at the IRSID (4) on a mild semi-killed manganese-silicon steel (UTS = 500 MPa), the influence of the filler metal strength was studied. It was observed that, on as-welded joints, the fatigue limit declined with filler-metal strength, while on flush welds the fatigue limit remained constant, slightly below the limit of the base metal. The fall in fatigue limit observed on as-welded joints can be explained by the increase in sensitivity to notch effect with the increase in filler-metal strength.

As-welded joints executed in mild steels or high-yield-strength steels result in similar $\Delta\sigma$ values, in the case of low mean stresses. In this case, the insignificant influence of the yield strength is chiefly due to the small length of the initiation phase in proportion to the total fatigue life of a welded joint with a high fatigue notch factor. The fatigue life in propagation is similar (cf. section 4.2.2) for all structural steels.

In practice however, an advantage is usually found in using steels with a higher yield strength.

High stresses. An improvement is noted in the fatigue strength of welded joints with increases in yield strength, whether in the field of high stress variations (limited fatigue strength) as shown in figure 23, or in the case of high mean stresses. The latter effect is schematically represented in figure 24. On a Goodmann-Smith diagram, the test results are located on straight lines with variations in mean stress σ_m. For low or nil mean stresses, the results are similar; on the other hand, the effect of the yield strength is observed with increases in σ_m.

Stresses of variable amplitude. Such stresses, when encountered on an operational structure, generally incorporate high stress cycles ($\Delta\sigma$, σm), even in small numbers. In this very common case it is often worthwhile using high-yield-strength steels.

Welded joints with a low K_t value. Figure 25 shows the favourable effect of an increase in the yield strength of the base plate, on the conventional yield strength $\Delta\sigma_{2.10^6}$ on an as-welded butt joint with a slight reinforcement.

As will be seen in section 5, post-welding treatments have the effect of improving the fatigue strength of welded joints, which increases with the yield strength of the base metal.

3.4 Nature of stresses

3.4.1 Loading mode

A comparison of the results obtained either under tensile or bending loading shows, in the case of full-penetration welds, an effect of the stress gradient in the vicinity of the weld toe, which results, in particular, in a plate thickness effect.

Moreover, a welded joint subjected to bending stress is much less sensitive to the effect of incomplete penetration than the same joint subjected to tensile stress.

This difference in behaviour can be explained by a different breakdown of local stresses, either at the weld toe or at the level of incomplete penetration (15).

3.4.2 Loading ratio ($R = \sigma_{min} / \sigma_{max}$)

The value of the stress ratio (or mean stress of the loading cycle) has some influence on fatigue characteristics (30).

Although it is generally hard to deduce, from tests performed for a certain value of R, data corresponding to another value of the loading ratio, the following ratios are generally used:

$$\frac{\text{fatigue strength amplitude } (R_s = -1)}{\text{fatigue strength amplitude } (R_s = 0)} = 1.25 \qquad (3)$$

$$\frac{\text{fatigue strength amplitude } (R_s = 0.5)}{\text{fatigue strength amplitude } (R_s = 0)} = 0.85 \qquad (4)$$

In this case, the fatigue strength amplitudes are determined for 2.10^6 cycles.

These ratios have been determined by means of tests carried out on small test specimens taken from real structures. As a result, the level of residual stresses in the test specimens is relatively low (or even nil) by comparison with a real structure.

In practice, when the presence of high residual stresses (close to σ_y) may be feared, and where it is possible neither to measure such stresses nor to perform a stress-relieving heat treatment, it is assumed that the maximum fatigue strength amplitude corresponds to the value determined on the Goodmann chart in accordance with the diagram reproduced in figure 26. This is why most of the present computation codes do not consider the mean stress effect and provide, for a given type of welded joint, a single value of acceptable stress range $\Delta\sigma$.

3.4.3 Complex stresses

Few of the results in the literature concern cases of complex loading. Such cases are, however, provided for in certain computation codes which propose purely and simply the application of procedures used for static stresses.

An approximate method consists in regarding the maximum main stress as a computation stress to be compared with the acceptable stress for the welded joint in question (31).

4. CRACK PROPAGATION IN WELDED JOINTS

4.1 Application of fracture mechanics

As we saw in section 3, the fatigue strength of a welded joint largely depends on the presence of surface shape defects or internal defects (porosity, lack of penetration). Much research shows that from such defects the stage of fatigue crack initiation may be reduced and that as a consequence a large part of the life of welded joints subjected to fatigue stress is in propagation.

For the design of such joints, therefore, it is worth applying the laws of crack propagation provided by fracture mechanics in order to estimate the joint lifetimes by calculating the number of cycles required to cause crack propagation from these defects through to fracture.

The principle for calculation of propagation times is then as follows.

The rate of propagation of a fatigue crack da/dN is simply expressed as a function of the range of the part's stress intensity factor, ΔK, by a law of the Paris type:

$$da/dN = C.\Delta K^m \qquad (5)$$

$$K = \Delta\sigma \sqrt{\pi a}.f(a) \qquad (6)$$

Where:

$\Delta\sigma$ is the variation in nominal stress applied to the structure, and
f(a) is a corrective factor allowing for the geometry of the structure and the loading conditions.

The total fatigue life of a welded joint is accordingly estimated by integration of the following law:

$$N_p = \int_{a_i}^{a_f} \frac{da}{C.\Delta K^m} = \frac{1}{C.(\Delta\sigma)^m} \cdot \int_{a_i}^{a_f} \frac{da}{\left[\sqrt{\pi a}.f(a)\right]^m} \qquad (7)$$

N_p is the number of propagation cycles for a joint containing an initial defect a_i on which failure occurs for crack length a_f. For a given joint, if a_i and a_f are adopted as constant, irrespective of the constant amplitude stress applied, the integral is a constant.

Relation (3) can be more simply expressed as follows:

$$N_p = C' \Delta\sigma^{-m} \qquad (8)$$

The relation is accordingly respresented by a straight line of slope (-1/m) in a chart (log $\Delta\sigma$ - log N_p).

To apply fracture mechanics to welded joints, then, one must know the law of propagation for the material and the expression of ΔK corresponding to the joint shape. ΔK can be calculated by the finite element method, although simplified analytic models are are often used with test specimens equivalent to the joints studied and for which the expression of ΔK is known.

The object of a recent bibliographic survey (32) was to sum up the conditions of application of fracture mechanics for various types of welded joint, specifying, in particular:
- the proposed solutions for determination of function f(a)
- the parameters allowed for in this analysis
- the accuracy of estimation of a structure's lifetimes.

The main conclusions of the study in question are summed up below.

4.2 Crack initiation rates in welds

4.2.1 Comparison of propagation rates

A comparison between crack propagation rates in HAZ or the weld metal and those in the base metal usually shows major deviations in the case of welded joints in the as-welded condition. These deviations are reduced and cancelled out as ΔK (K_{max}) increases, for a high R value and after stress-relieving heat treatment.

The essential role played by the sampling technique is shown in figure 27; depending on the sampling technique, either higher or far lower propagation rates can be obtained.

4.2.2 Influence of yield strength

During the second stage of stable propagation of the fatigue crack, a slight increase in m with, at the same time, a reduction in C, is observed with increases in yield strength. In actual fact, in view of the relation $C = A/B^m$ proposed by Gurney (33) and confirmed by Lieurade (34) (figure 28) for results obtained in the base metal, HAZ and weld metal on test specimens less than 20 mm thick, only the evolution of m need be watched.

Figure 29 shows a slight decrease in m with decreases in the yield strength.

4.2.3 Role of residual stresses

The problems frequently encountered in interpreting the results of crack propagation tests on test specimens taken from welds are usually due to the variety of the residual stress field set up initially during welding and subsequently in part subjected to stress-relieving heat treatment during the taking and machining of test specimens.

This is why, in order to express the test results, various authors determine, either by measurement or calculation, the residual stress field in the test specimens tested, and the evolution of this field as the crack progresses.

In this way it is demonstrated that the residual stress level increases with the yield strength and plate thickness. The effect of residual stresses tends to be cancelled out as R increases.

Another way of regarding the effect of residual stresses is to measure parameter ΔK_{eff} corresponding to the part of the loading cycle during which the crack is fully open. Figure 30 shows that, by applying this parameter, the results obtained on the base metal for R = 0.7 can be superimposed on the results determined in the HAZ for R = 0.1. In practice, irrespective of the stress conditions (R, residual stresses), a single curve can be obtained by considering only that portion of the cycle during which the crack is fully open.

4.3 Crack propagation at the weld toe

The evolution of stress intensity factor, K, corresponding to a crack initiated in the weld toe and propagated through the thickness of the plate, was calculated in the case of fillet welds (35), butt joints (36) and tubular joints.

By way of example, we shall consider the case of fillet welds, for which Maddox (37) assumes a defect of semi-elliptical surface for semi-axes a and c (figure 31). The stress intensity factor obtained by finite element analysis, is of the following form:

$$K = \sigma \sqrt{\pi a}\, \frac{M_s . M_t . M_k}{\omega_0} \qquad (9)$$

Where:
- M_s = free surface correction
- M_t = finite thickness correction
- M_k = correction due to stress concentration
- ω_0 = form factor

$$\omega = \int_0^{\pi/2} \left[1 - \left(1 - \frac{a^2}{c^2}\right) \sin^2 \varphi \right]^{1/2} d\varphi \qquad (10)$$

for a highly elongated defect ($\frac{a}{c} = 0$), $= 1$

Factor K was calculated for a cruciform joint and an elongated defect ($\omega_0 = 1$) as a function of a/B (B = plate thickness) and for variable transition angles θ.

For $\theta = 0$, $K = \sigma \sqrt{\pi a} \left[1.22 - 0.231\left(\frac{a}{B}\right) + 10.55\left(\frac{a}{B}\right)^2 - 21.7\left(\frac{a}{B}\right)^3 + 33.19\left(\frac{a}{B}\right)^4 \right]$ (11)

For $\theta \neq 0$, there exists a stress concentration in the weld toe and the value of K is higher in the vicinity of a/B = 0 (figure 32).

4.4 Crack propagation from welding defects

Crack propagation from porosity, nonmetallic inclusions and lack of penetration has been examined by various authors. Here we shall examine the case of a lack of penetration in a cruciform joint.

This type of defect, similar to a crack in nature, is an exemplary case of application of the concepts of fracture mechanics.

For this type of defect, Frank (38) has determined a K solution specifically adapted to the root of a cruciform weld, using finite element techniques. This solution is used by Maddox (39) in the following form:

$$K = \frac{\sigma_p}{1 + 2H/Tp} \left[A_1 + A_2\,(a/w) \right] \left[\pi a \sec \frac{(\pi a)}{2w} \right]^{1/2} \qquad (12)$$

Where: σ_p, H, Tp, a and w are as defined on figure 33
A_1 and A_2 are polynomials of H/T_p.

Using this expression of K, the integration of the law of the crack propagation rate (with m = 3) leads to an expression of the following form:

$$I = C\, w^{1/2}\, (\Delta \sigma_p)^3\, N \qquad (13)$$

Where: I is an integral whose evolution as a function of a_i/w, for given values of H/Tp, is specified on figure 33.

5. IMPROVEMENT OF WELDED-JOINT FATIGUE STRENGTH

As was indicated in section 3.3.4, high-yield-strength steels are now increasingly used in the execution of welded structures.

A number of studies have shown the advantages of HYS steels in the execution of welded structures, especially in the case of high mean stress levels or loading at variable stress amplitudes. On the other hand, comparison of the results of fatigue tests on welded structures in conventional conditions (low or nil mean stress, constant stress amplitude) shows no significant advantage for HYS steels.

This phenomenon is usually explained by the short time for fatigue crack initiation due to the inevitable presence of defects in the weld toe of as-welded joints. At the same time, the phenomenon is explained by the slight variation observed in the crack propagation rate as a function of the yield strength of structural steels, which leads to similar crack initiation times.

It therefore became apparent that the only way of taking full advantage of high-yield-strength steels was to increase the crack initiation time in relation to the total life of a welded joint. For this purpose, various techniques can be used. The object of such techniques is to alter the weld's macrogeometry (weld profile) and microgeometry (welding defects) and

the residual stress field set up by the welding operation. The techniques in question can only be applied to cases where crack initiation takes place in the weld toe.

The techniques are discussed in recent bibiographic surveys (40),(41).

5.1 Alteration of weld geometry

Geometry of the weld toe

For automatic welding processes, the welding parameters should be set so as to reduce to a minimum the weld reinforcement (butt joint) and obtain as large as possible a transition radius between the weld bead and the plate.

The latter recommended requirement can be obtained by using improved coated electrodes (42) during the weld toe run.

Weld geometry and welding sequence

Figure 34 shows the improved procedure used in the case of Tee joints subjected to bending stresses.

The general profile of the weld promotes a good stress flow, thereby reducing the joint's K_t level.

The proposed welding sequence (43) which consists in making the weld toe run just after the root runs has several advantages. The sequence facilitates positioning of the weld toe; the flat run gives optimum wettability and accordingly a large transition radius. This run undergoes stress-relieving heat treatment by the filling runs, resulting, on the one hand, in reduced underbead hardness, while at the same time cancelling out the residual stresses in the weld toe. Figure 35 compares the results achieved by a standard procedure and by the improved procedure (43).

5.1.2 Dressing of the weld toe

TIG dressing

Postwelding treatment by the TIG process consists in dressing of the weld transition zones by means of a TIG torch, without filler metal. The process provides a reduction in the stress concentration, by levelling the weld profile (figure 36) at the transition level and by increasing the hardness in the treated zone. The results achieved are spectacular, especially in the case of fillet welds, which usually have the highest stress concentration. Figure 37 shows that the rates of improvement in the conventional fatigue limit achieved in this case increase rapidly with the base plate's yield strength.

Plasma dressing

The principle of the method is similar to the TIG dressing process. The main difference is due to the heat applied, which is twice as great in the case of plasma dressing, allowing faster welding speeds. The rates of improvement are of the same order as for TIG dressing.

5.1.3 Weld toe grinding

By means of this technique, incipient cracks are eliminated by removing metal from the weld toe. This machining operation can be performed either by disc grinder or with a grinding mill (figure 38). To eliminate all slag inclusions and microcracks, the machining depth should be 0.5 to 0.8 mm. At the same time as it eliminates incipient cracks, the technique also allows improvement of the weld profile and a consequent reduction in the local stress concentration factor.

The results achieved by this technique largely depend on the care with which the operation is performed. The rates of improvement in the conventional fatigue limit range between 30 and 100%.

5.2 Alteration of the residual stress condition

5.2.1 Weld toe hammer-peening

By this technique, major residual compressive stresses are set up on the skin by pneumatic hammer. Existing defects are not eliminated, but their shape is altered. After hammer-peening, these defects are surrounded by a volume of cold-worked material where high compressive stresses prevail.

The hammer can be equipped with an hemispherical-head tool or a needle device. The effectiveness of hammer-peening depends on the number of runs or the length of the operation. The results obtained by this method are remarkable: the improvement is twice as great as that obtained by TIG dressing.

5.2.2 Shot peening

In shot peening, the surface to be treated is bombarded with calibrated steel shot. Each impact of the shot has the effect of a small hammer blow. This treatment allows a residual compressive stress field greater than 0.5 σ_y to be set up in the surface layer. The level of the stress set up, its uniformity in all respects, and the depth of the prestress layer, are reproducible and depend on a number of parameters which should be verified: shot diameter, bombardment time and energy, nozzle diameter, distance and angle between the nozzle and the part, rate of displacement, etc.

Few results can be found in the literature. Figure 35 shows the remarkable improvement obtained when shot peening treatment is applied to Tee joints.

Measurement of the evolution of residual stresses as a function of $\Delta\sigma$ or N shows (44) that in the region of the fatigue limit, no relaxation of residual stresses is observed. In this case, the stresses can be schematically regarded (figure 39) as static stresses which are algebraically added to the mean stress of the cyclic load.

5.3 Summary of results

5.3.1 Estimate of crack initiation time

Using strain gauges placed on the weld toe (43) or an AC potential drop method, it was possible to estimate the crack initiation time.

The results show that, by improvement treatments, a crack initiation phase can be introduced which lasts at least half the joint's lifetime (figures 35 and 40).

5.3.2 Comparison of improvement techniques

A statistical study concerning numerous results in the literature (45) showed the following mean rates of improvement:

- grinding 49%
- hammer- and shot-peening 57%
- TIG or plasma dressing 83%

In that study, the results were analyzed without taking into account the influence of various parameters such as welded-joint geometry, plate thickness, ratio R, and the steel's yield strength.

6. LOADING AT VARIABLE AMPLITUDES

6.1 Stress distribution

Welded structures are usually subjected to operating loads of variable amplitudes. To allow for this type of loading when designing a structure, various stages must be gone through (46).

- The evolution of nominal stresses on structures of the same type subjected to operating stresses is recorded.
- The spectra recorded are analyzed. Various methods proposed in the literature (47) allow definition of a characteristic stress distribution for a type of structure (e.g., cranes, bridges, and offshore structures).
- A law of damage is used, or else simulation tests are performed in lab, using the stress distribution obtained.

6.2 Law of damage

To allow for stress amplitude variations, a law is usually applied which specifies the contribution of each cycle to structural damage.

Palmgren and Miner's hypothesis, by which the cumulative damage is calculated linearly, is most frequently used. In practice, the sum of elementary ratios n_i/N_i is calculated (where n_i is the number of cycles undergone at a stress level σ_i for which the lifetime is N_i - figure 41).

According to Palmgren and Miner, when cycles of different amplitudes are involved, failure should occur when the sum of the fractions of life corresponding to each level is equal to unity:

$$\Sigma \frac{n_i}{N_i} = 1 \qquad (14)$$

While this extremely simple law has been verified in certain cases, one observes that it is not general and that the initial hypothesis is not true. In particular, the damage is not governed by a single parameter. It has been found that the damage undergone by a test specimen or part depends not only on the number of cycles at each level, but also and above all on the order of succession of stress levels.

Nevertheless, in spite of these imperfections, this law is widely used, with the value of $\Sigma n_i/N_i$ being generally set at less than 1 to allow a safety margin.

6.3 Lab simulation tests

The stress amplitude distribution can be directly applied to welded-structure members. To allow for a distribution set characteristic of a type of structure, a parametric representation can be used.

Figure 42 shows by way of example the various shapes that can be adopted by the distributions in relation to hoisting machinery, and the value of the relevant parameter p.

The "programmed block" method (figure 43) consists (48) in breaking down the distribution studied into a number of plateaus corresponding to a constant stress amplitude. The test sequence is subsequently formed of sub-plateaus in such a way that the same plateau does not occur continually for too long, but the frequency is complied with.

Figure 44 shows the system of Wöhler pseudo-curves obtained for three values of parameter p. Other simulation methods are proposed (47) in order to reproduce stresses of variable amplitude; these methods generally require more sophisticated test facilities.

7. CONCLUSION

However complex it may be, a steel structure generally consists of a small number of various joints. To learn the structure's fatigue strength, the fatigue strength of the various joints can be studied separately.

Welded-joint fatigue strength is affected by many factors, chief of which is the quality of the weld. The fatigue strength of welded joints is especially sensitive to the geometry of the weld bead and the stress fields set up, as a result either of the welding process or the microscopic effects incorporated in the weld. To improve their fatigue behaviour, the welds may be subjected to mechanical or heat treatments.

It is possible to find out accurately the characteristics of welded joints subjected to cyclic stresses, by means of lab simulation tests carried out on industrially welded test specimens of sufficient size to be representative of the members of a real structure.

On the basis of such tests carried out at constant or variable loading amplitude, the acceptable stresses corresponding to a given structure life and an estimated distribution of stresses applied to the joint in service are then defined for each type of welded joint.

1. Harrison, J.D., Welding Research Int. (1971), 1, No. 1.

2. Lieurade, H.-P., Gerald, G., Proc. Int. Conf. on Steel in Marine Structures, pages 6.4, Paris (1981).

3. Doc. IIS/IIW - 693 - 81.

4. Rabbe, P., Bastenaire, F., Granjon, H., Soudage et Techniques Connexes (1968) No. 5/6, 205-211.

5. Kenyon, N., Morison, W.B., Quarrel, A.G., British Welding Journal (1966), 3, 123-137.

6. Lawrence, K.V., Welding Research Supplement (1973), 212 s.

7. Sanders, W.W., de Rech, A.T., Munse, W.H., Welding Research Supplement (1965), 2, 49s - 55s.

8. Yamaguchi, I., Terada, Y., Nitta, A., IIS/IIW Document XIII 425-66.

9. Nishida, M., Stress Concentration, Morikita Pub. Co. (1967).

10. Williams, H.E., Ottsen, H., Lawrence, F.V., Munse, W.H., Civil Engineering Studies. Structural Research Series No. 366, Univ. of Illinois (1970).

11. Richards, K.G., Fatigue Strengtn of welded structures. The Welding Institute, (1969).

12. Watkinson, F., Bodger, P.H., Harrison, J.D., Proc. Conference to Brighton (1970), The Welding Institute (1971), 97-113.

13. Petershagen, Doc. IIS/IIW XIII - WG4-15-83.

14. Gurney, T.R., Fatigue of Welded Structures, Cambridge University Press, (1979).

15. Bignonnet, A., Doc. IIS/IIW - XIII - 1098-83.

16. Maddox, S.J., Private Communication.

17. Ryan, I., Recho, N., Régnier, L., Lieurade, H.-P., Proc. Int. Conf. of Welding of Tubular Structures, Boston (1984).

18. Maddox, S.J., Doc. IIS/IIW - XIII - WG4-18.84.

19. Rules for the Design, Construction and Inspection of Offshore Structures. Appendix C., Steel Structures. DnV (1977), C32-C35.

20. Newman, R.P., Dawes, M.G., British Welding Journal (1965), 3, 117-120.

21. Newman, R.P., BWRA Bulletin (1961), 18-21.

22. Gurney, T.R., Smith, G.C., British Welding Journal (1967), 1, 17-38.

23. Harrison, J.D., Gurney, T.R., British Welding Journal (1967), 3, 121-131.

24. Erdmann-Jesnitzer, F., Klaas, H., Muller, S., Sweisstechnik (1956), Vol. 6, 133-139.

25. Stager, H., Held, F., Schweiz. Archiv Angewandte Wiss. u. Techn. (1945), 11, 361-385.

26. Harrison, J.D., Smith, G.C., British Welding Journal (1967), 9, 493-502.

27. Ishii, Y., Iida, K., J. of Soc. of NDT (1969), 18, Doc. IIS/IIW - XIII - 560 - 69.

28. Harrison, J.D., Metal Construction and British Journal (1972), 99-107. Doc. IIS/IIW - XIII - 624-71.

29. Matting, A., Neitzel, M., British Welding Journal (1967), 1, 3-7.

30. Lieurade, H.-P., Metaux - Corrosion - Industrie (1974), 586, 1-24.

31. Harrison, J.D., Private Communication.

32. Lieurade, H.-P., Welding in the World, 1983, Vol. 21, 272-295. Doc. IIS/IIW - 756-83.

33. Gurney, T.R., Welding Research Int., 1979, Vol. 9, 4, 45-59.

34. Lieurade, H.-P., Maillard-Salin, C., Truchon, M., IABSE Colloquium, Lausanne (1982), 137-144.

35. Harrison, J.D., Welding Research Int., 1, No. 1 (1971).

36. Lawrence, F.V., Munse, W.H., Welding Journal (1973), 52, No. 5, 221s - 225s.

37. Maddox, S.J., Int. J. of Fracture, 11, (2), (1975), 221.

38. Frank, K.H., The Fatigue Strength of Fillet Welded Connections. Ph.D Thesis, Lehig University (1971).

39. Maddox, S.J., Weld. J. Research Supp. (1974), 401s-409s.

40. Haagensen, P.J., Int. Conf. on Steel in Marine Structures, Paris (1981) Plenary Session 6.

41. Bignonnet, A., Doc. IIS/IIW - XIII - 1085-83.

42. Kobayashi and coworkers. Doc. IIS/IIW - XIII - 828-77.

43. Bignonnet, A., Lieurade, H.-P., Picouet, L., Int. Conf. of Welding of Tubular Structures, Boston (1984).

44. Picouet, L., Bignonnet, A., Lieurade, H.-P., 2nd Int. Conf. on Shot Peening, Chicago (1984).

45. Olivier, R., and Ritter, W., Int. Conf. on Steel in Marine Structures, Paris (1981) pages 9-6.

46. Lieurade, H.-P., La fatigue des matériaux et des structures, Ed. Maloire (1980), 343-379.

47. Strating, J., Fatigue and Stochastic Loadings, Delft University of Technology.

48. Gassner, E., Griese, F.W., and Haibach, E., Arch. Eisenhüt., 35 (1964), 255-267.

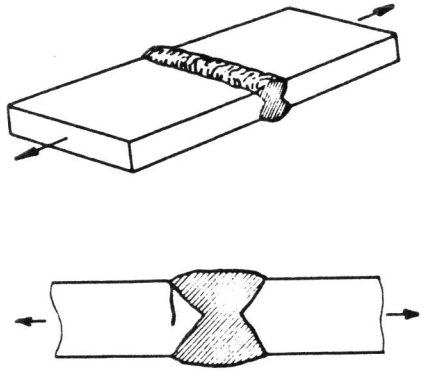

Fig. 1 - Transverse butt joint.

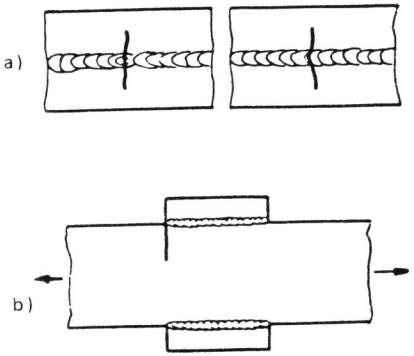

Fig. 2 - Longitudinal butt welds.
a) crack initiation at run stops
b) crack initiation at weld end.

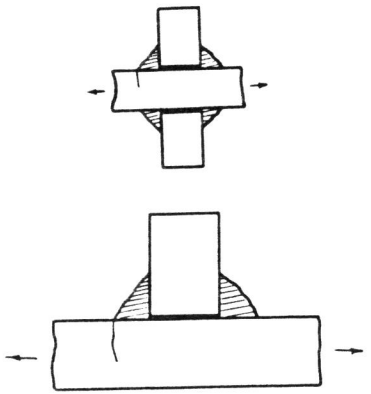

Fig. 3 - Transverse non-load-carrying fillet welds (crack initiation at the weld toe.

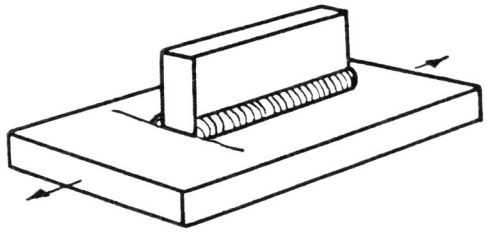

Fig. 4 - Longitudinal fillet weld. (initiation at the weld end).

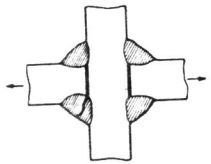

Fig. 5 - Transverse load-carrying fillet weld (crack initiation at the weld root).

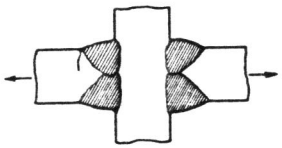

Fig. 6 - Cruciform joint with full penetration (crack initiation at the weld toe).

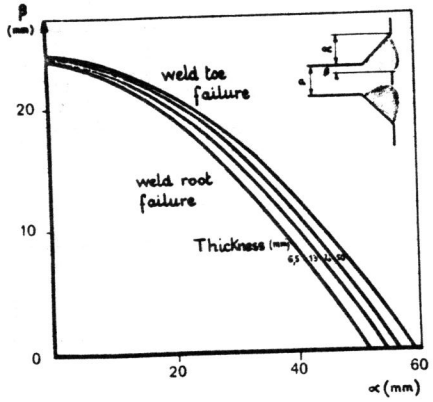

Fig. 7 - The effect of the weld geometrical conditions on the initiation site in the case of a lack of penetration.

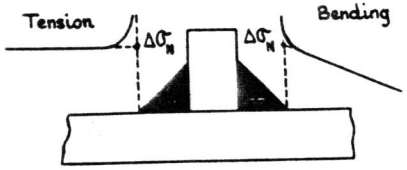

Fig. 9 - Definition of the nominal stress range, $\Delta\sigma_N$, in the case of a transverse fillet weld.

joint configuration	Description	$\Delta\sigma_{2.10^6}$ (MPa)
	transverse butt weld ground flush to plate 100 % NDT	125
	transverse butt welds NDT	100
	cruciform joint K-butt weld with fillet welded endo misalignment ≤ 15 % t (t: plate thickness)	71
	load carrying fillet welds (root failure)	45

Fig. 11 - Classification of joints (3).

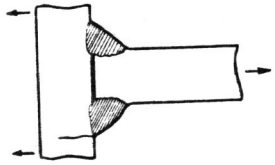

Fig. 8 - Tee Joint.

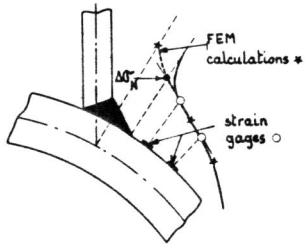

Fig. 10 - Definition of $\Delta\sigma_N$ at the hot spot of a tubular connection.

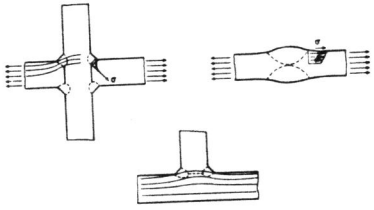

Fig. 12 - Stress concentration zones on welded joints.

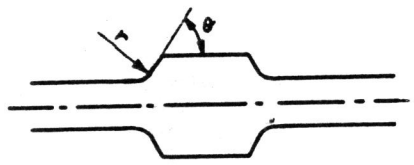

Fig. 13 - Geometrical parameters of simulated joints.

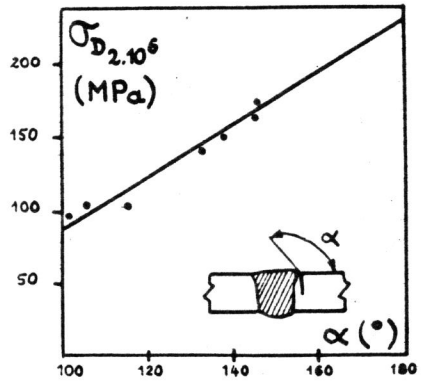

Fig. 14 - The influence of the transition angle on the fatigue limit at 2.10^6 cycles (butt joint)(8).

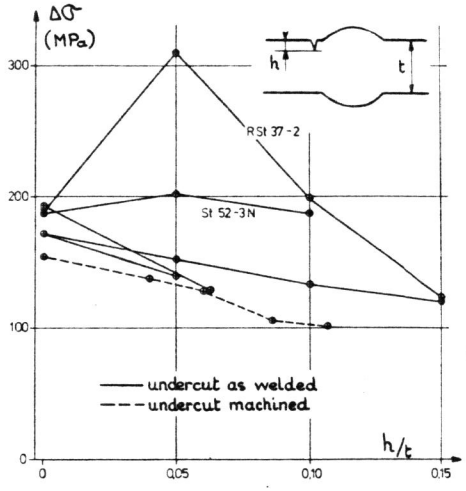

Fig. 15 - Stress range for butt welds in steel, plotted against h/t .

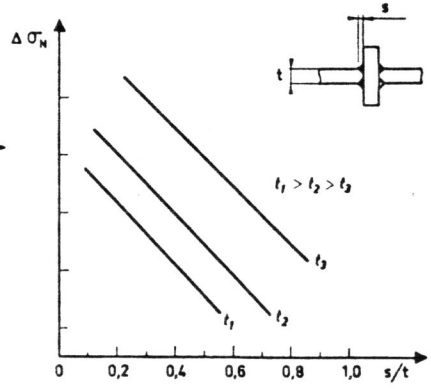

Fig. 16 - The schematic influence on s/t (s : bead width, t : plate thickness) on the fatigue strength.

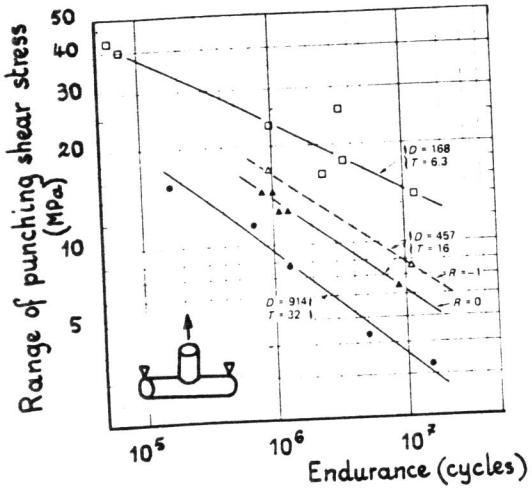

Fig. 17 - The influence of the plate thickness and the chord diameter on the fatigue strength in the case of tubular nodes.

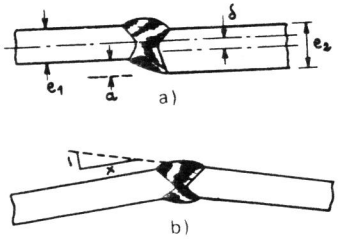

Fig. 18 - Misalignments.

a) axial
b) angular

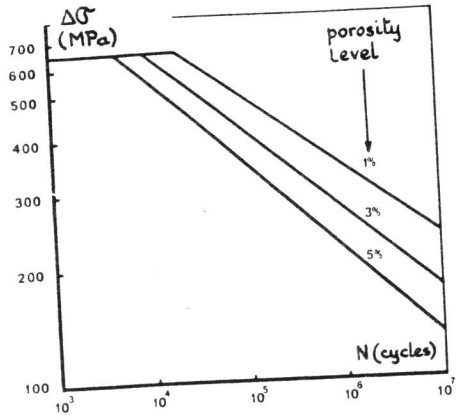

Fig. 19 - The effect of porosity on the fatigue strength - butt joints - (27).

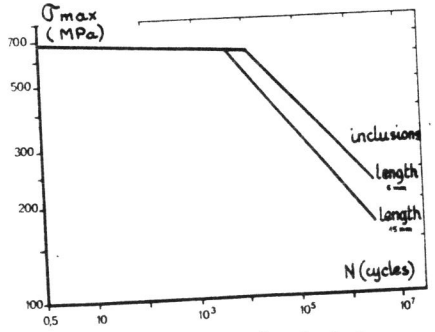

Fig. 20 - The effect of slag inclusions on the fatigue strength - butt joints - (27).

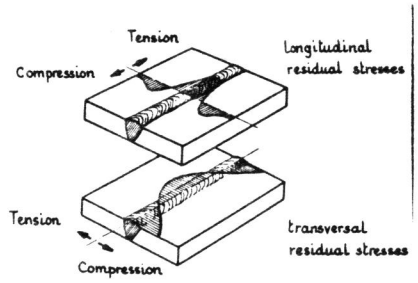

Fig. 21 - Residual stress field due to the weld process.

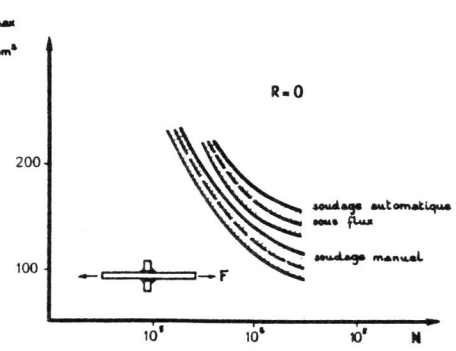

Fig. 22 - The effect of the welding process on the fatigue strength of non-load-carrying fillet welds.

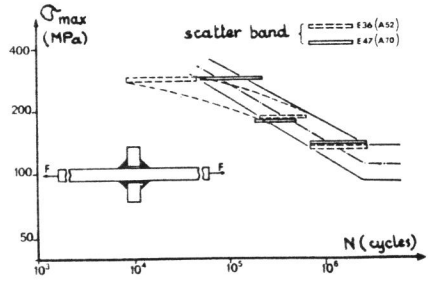

Fig. 23 - The effect of the plate yield point (360 or 470 MPa) on the fatigue resistance of cruciform joints.

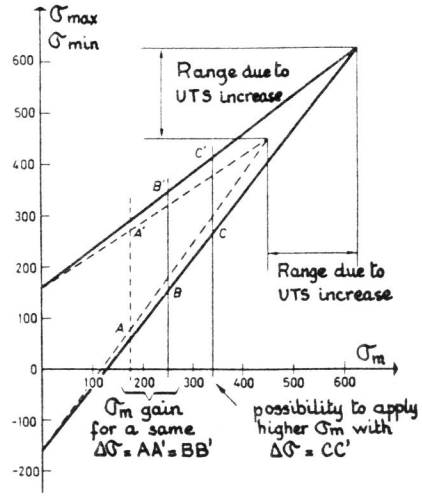

Fig. 24 - The schematic increase in fatigue resistance with UTS (or σ_y) for high σ_{mean} level.

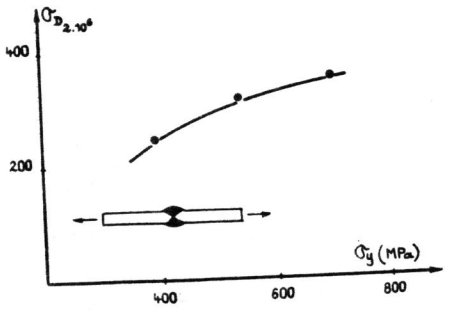

Fig. 25 - The effect of the plate yield point on the fatigue resistance of transverse butt joints - R = 0 - (from RABBE and coworkers).

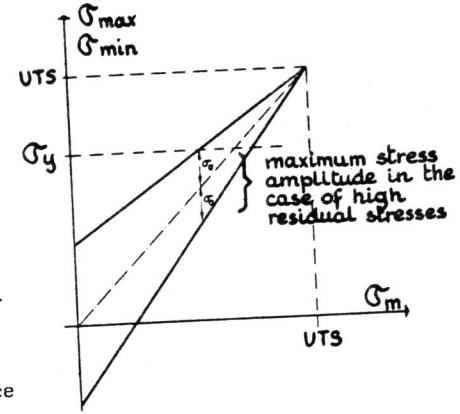

Fig. 26 - Schematic determination of the fatigue strength in the case of high residual stresses.

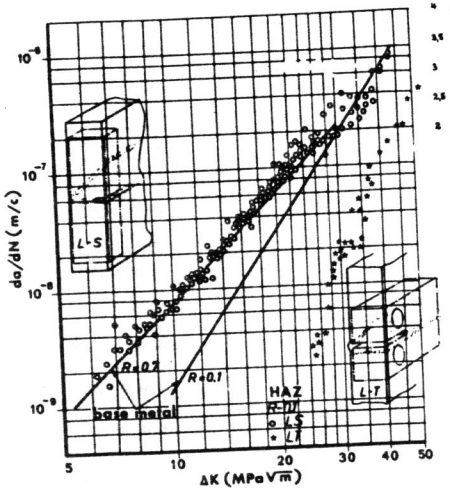

Fig. 27 - The influence of crack growth direction on fatigue crack growth rate in HAZ (R = 0.1)(34).

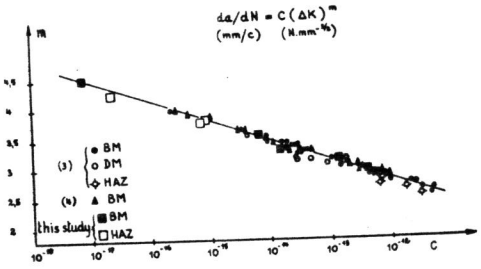

Fig. 28 - m vs C (34).

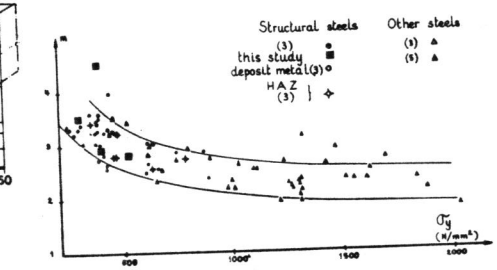

Fig. 29 - m vs σ_y (34).

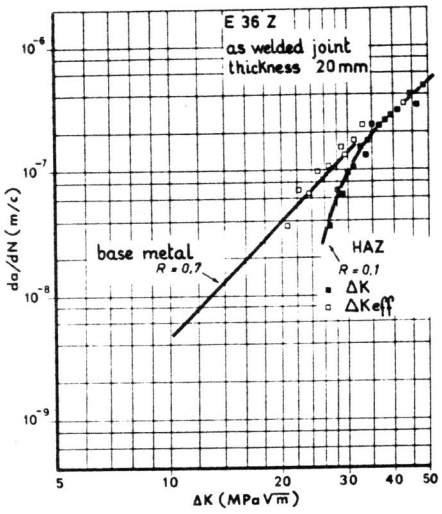

Fig. 30 - da/dN vs ΔK or ΔK_{eff} in HAZ (34).

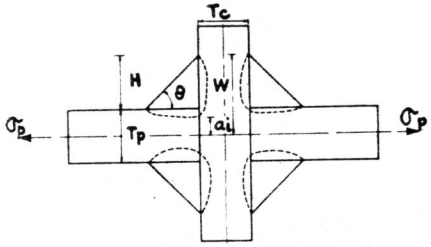

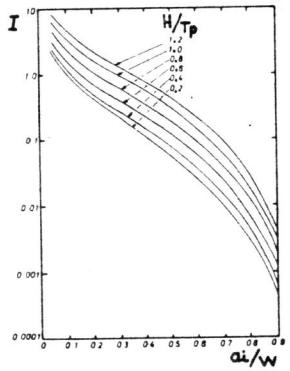

Fig. 33 - Crack propagation integral for weld crack in cruciform joint as a function of initial flaw size (from (39)).

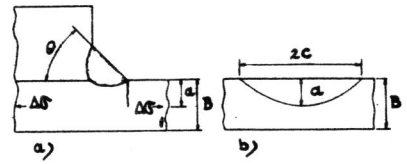

Fig. 31 - Details of weld toe crack.
a) section
b) plane of fracture (from (37)).

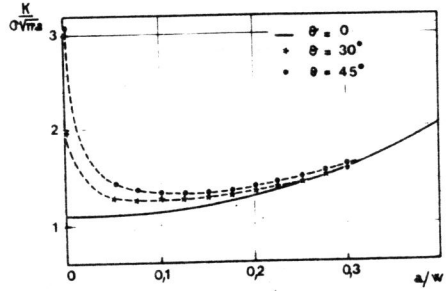

Fig. 32 - Influence of a/W and θ on K (non-load-carrying fillet weld) (from (37)).

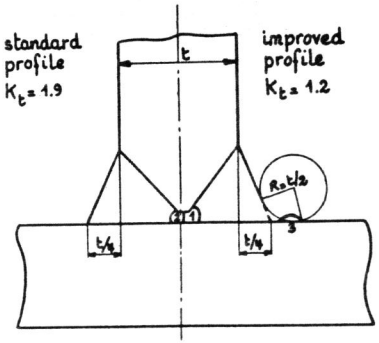

Fig. 34 - Comparison of the standard profile and a improved profile in the case of offshore constructions.

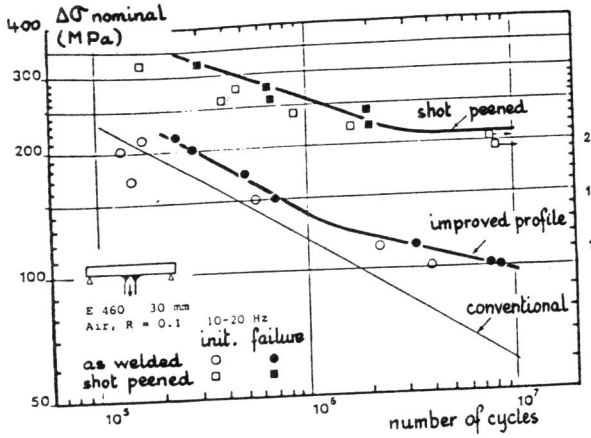

Fig. 35 - The influence of an improved bead profile, as welded or shot peened on the fatigue strength of Tee joints.

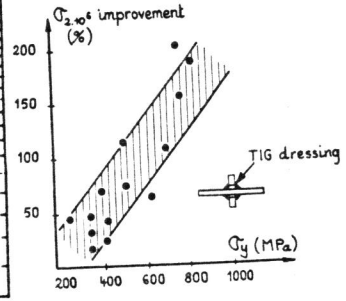

Fig. 37 - Fatigue strength improvement due to TIG dressing, as a function of σ_y.

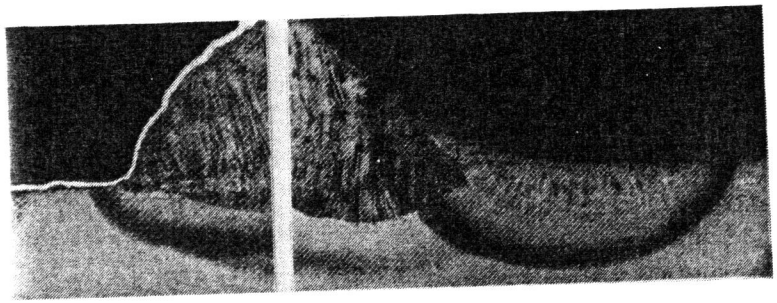

a) as welded. b) after TIG dressing.

Fig. 36 - The influence of TIG dressing on the weld bead profile.

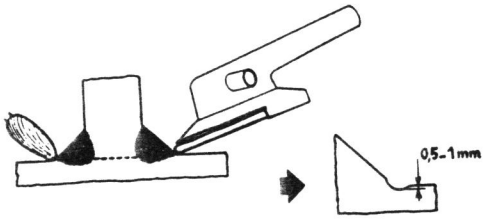

Fig. 38 - Grinding of the weld toe.

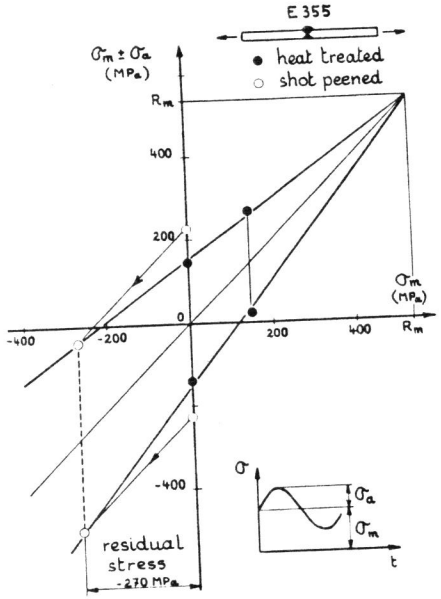

Fig. 39 - Role of the residual stresses due to shot peening on the fatigue strength of butt joint.

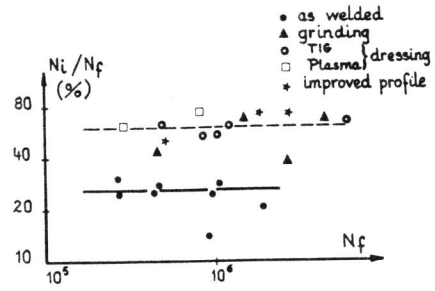

Fig. 40 - The influence of post weld treatment on the fatigue crack initiation period.

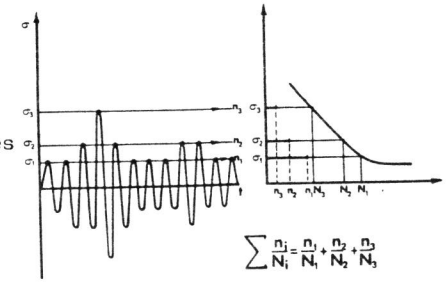

Fig. 41 - Schematic application of the Palmgren-Miner rule.

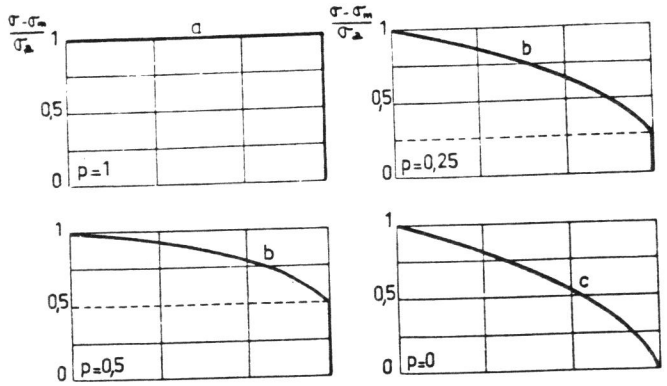

Fig. 42 - Various loading distribution shape in the case of lifting structures.

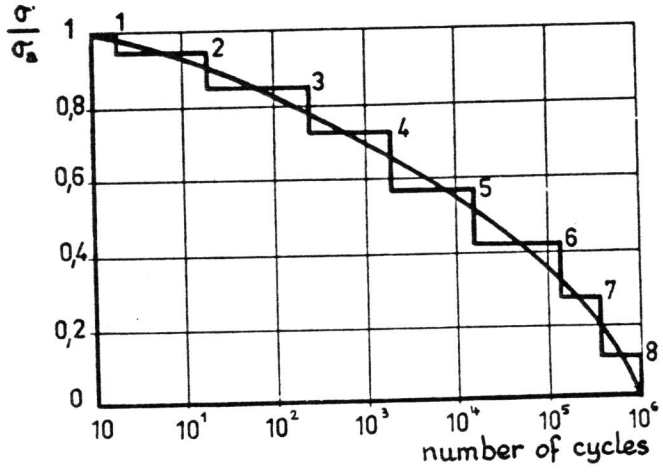

Fig. 43 - Loading distribution breaking down into 8 blocks.

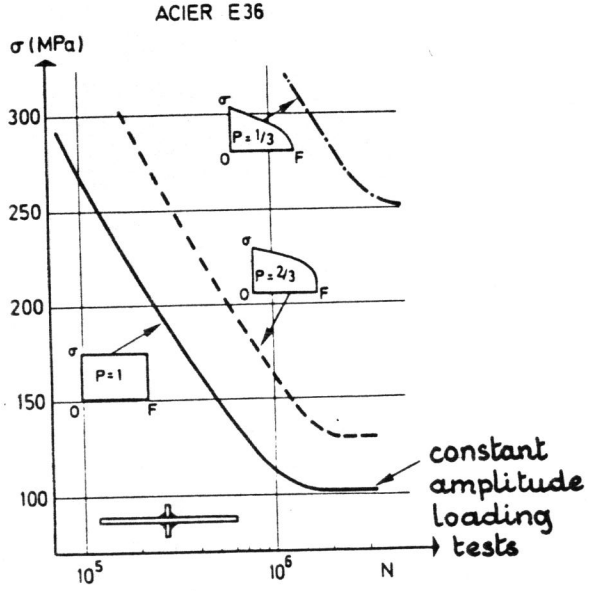

Fig. 44 - Fatigue test results using the "programmed block" method(30).